Berlin, 1985).
3. B. Hess, A. Boiteaux, J. Kruger, *Adv. Enzyme Regul.* **7**, 149 (1969).
4. B. Hess and A. Boiteaux, *Hoppe-Seyler's Physiol. Chem.* **349**, 1567 (1968).
5. C. L. Slayman, W. S. Long, D. Gradmann, *Biochim. Biophys. Acta* **426**, 732 (1975).
6. S. R. Caplan *et al.*, *Nature* **245**, 364 (1973).
7. M. Schell, K. Kundu, J. Ross, *Biophysics* **84**, 424 (1987).
8. Y. Termonia and J. Ross, *Proc. Natl. Acad. Sci. U.S.A.* **78**, 2952 (1981); *ibid.*, p. 3536; *ibid.* **79**, 2878 (1981).
9. J. M. Douglas and D. W. T. Rippen, *Chem. Eng. Sci.* **21**, 305 (1966).
10. V. P. Skulachev and P. C. Hinkle, Eds., *Chemiosmotic Proton Circuits in Biological Membranes* (Addison-Wesley, Reading, MA, 1981).
11. O. Kedem and S. R. Caplan, *Trans. Faraday Soc.* **21**, 1897 (1965).
12. F. Oster, A. S. Perelson, A. Katchasky, *Q. Rev. Biophys.* **6**, 1 (1973).
13. J. Schnakenberg, *Thermodynamic Network Analysis of Biological Systems* (Springer, New York, 1977).
14. H. Degn and L. F. Olsen, *Ann. N.Y. Acad. Sci.* **316**, 623 (1979).
15. I. Yamazaki, T. Ishikawa, M. Nakamura, K. Yokota, S. Nakamura, in *Biological Rhythms and Their Central Mechanism*, M. Suda, O. Hayaishi, H. Nakagawa, Eds. (Elsevier/North-Holland, Amsterdam, 1979), pp. 19–28.
16. I. Yamazaki and K. Yokota, in *Biological and Biochemical Oscillations*, B. Chance, E. K. Pye, A. K. Ghosh, B. Hess, Eds. (Academic Press, New York, 1973), pp. 109–114.
17. Glucose-6-phosphate dehydrogenase from Leuconostoc Mesenteroides can utilize both NAD^+ and $NADP^+$ as substrates.
18. The O_2 flux from the gas flow into the solution is a critical parameter in these experiments. The flux of O_2 into solution can be described by $dO_{2(sol)}/dt = k[flux_{(gas)}]$, where k is the rate constant for O_2 dissolution and $flux_{(gas)}$ is the flux of gaseous O_2 bubbling into the solution; k can be varied by using a fritt or gas diffuser and $flux_{(gas)}$ can be changed by changing the flow rate of the gas input. As long as the product of these two parameters remains the same, the behavior of the system and the results of these experiments remain the same. A run is started by adding 10 units of glucose-6-phosphate dehydrogenase (from Leuconostoc Mesenteroides) to a 4-ml reaction mixture containing 1.5 mmol/liter NAD, 25 mmol/liter glucose-6-phosphate, 100 unit/ml HRP, 1 μmol/liter methylene blue, 50 μmol/liter 2,4 dichlorophenol in a sealed 5-ml Reacti-vial. The reaction is brought to a steady state with a constant 3 ml/s flow of 3 mole percent O_2/N_2 delivered through a needle and bubbled through the solution. A small amount of the solution is continuously pumped through a flow cell in the spectrophotometer so that continuous absorbance measurements may be obtained.
19. K. Tornheim and J. M. Lowenstein, *J. Biol. Chem.* **248**, 2670 (1973); *ibid.*, p. 3241; *ibid.* **250**, 6304 (1975). Intracellular concentrations of ATP have been observed to vary by a factor of 3.
20. The thermodynamic cost of providing the O_2 perturbation has been calculated to be negligible (less the 0.05% of D).
21. N. J. Oppenheimer, *Coenzymes Cofactors* **2**, 185 (1987).
22. The rate of reaction 2 is measured by running an identical experiment without HRP. The reaction rate is effectively constant over the time course of data collection because the enzyme is saturated with respect to glucose-6-phosphate. The product of reaction 2, 6-phosphogluconolactone, is unstable and rapidly breaks down, thus preventing the accumulation of product. Furthermore, experiments performed with significantly more or less glucose-6-phosphate did not change the reaction rate.
23. A. Hjelmfelt and J. Ross, *J. Chem. Phys.* **90**, 5664 (1989).
24. M. A. McKarnin, L. D. Schmidt, R. Aris, *Chem. Eng. Sci.* **43**, 2833 (1988).
25. D. Juretic and H. V. Westerhoff, *Biophys. Chem.* **28**, 21 (1987).
26. J. Ross and M. Schell, *Annu. Rev. Biophys. Chem.* **16**, 401 (1987).
27. J. F. Hervagault, J. G. Lazar, J. Ross, *Proc. Natl. Acad. Sci. U.S.A.* **86**, 9258 (1989).
28. Supported in part by grants from the National Science Foundation and the National Institutes of Health.

24 July 1989, accepted 7 November 1989

Mountains and Arid Climates of Middle Latitudes

S. MANABE AND A. J. BROCCOLI

Simulations from a global climate model with and without orography have been used to investigate the role of mountains in maintaining extensive arid climates in middle latitudes of the Northern Hemisphere. Dry climates similar to those observed were simulated over central Asia and western interior North America in the experiment with mountains, whereas relatively moist climates were simulated in these areas in the absence of orography. The experiments suggest that these interior regions are dry because general subsidence and relatively infrequent storm development occur upstream of orographically induced stationary wave troughs. Downstream of these troughs, precipitation-bearing storms develop frequently in association with strong jet streams. In contrast, both atmospheric circulation and precipitation were more zonally symmetric in the experiment without mountains. In addition, orography reduces the moisture transport into the continental interiors from nearby oceanic sources. The relative soil wetness of these regions in the experiment without mountains is consistent with paleoclimatic evidence of less aridity during the late Tertiary, before substantial uplift of the Rocky Mountains and Tibetan Plateau is believed to have occurred.

THE MECHANISMS CONTROLLING the distribution of the earth's arid climates are only partially understood. While the existence of subtropical deserts can be explained by their location beneath the subsiding branch of the Hadley circulation, mid-latitude aridity is more problematic. Sizable dry regions stretch across the interior of Asia from Turkestan east to the Gobi Desert and across North America from the Great Basin to the western Great Plains. Some climatologists have speculated that distance from oceanic moisture sources is the major cause of such mid-latitude dry regions, accentuated locally by the presence of mountain barriers upwind (*1*). If this were the case, such dry regions would occur even in the absence of orography.

One way to separate the effect of orography on climate from other effects is through the use of atmospheric general circulation models (GCMs). In a number of studies, GCMs have been used to simulate the earth's climate with and without mountains (*2*). Most of these studies concentrated on the effects on atmospheric circulation, with less attention given to changes in the global distribution of climate brought about by the presence of mountains. Manabe and Terpstra (*3*) briefly discussed the impact of orography on the precipitation distribution, on the basis of simulations of the January climate with and without mountains. In their simulations, a zonal belt of moderate precipitation formed in the mid-latitudes of the Northern Hemisphere in the case without mountains, but interruptions in the belt over the interiors of Eurasia and North America developed in their experiment with orography. In a subsequent study using a model with orography and incorporating seasonal variation, Manabe and Holloway (*4*) compared the simulated and observed distributions of global climate. Their model simulated the mid-latitude dryness of the Eurasian interior, and they suggested that the presence of the Tibetan Plateau is important in maintaining central Asian aridity.

Recently, a series of studies was conducted in which large-scale uplift of the Tibetan Plateau and the western United States was linked to the changes in climate during the past 30 to 40 million years (*5–7*). As part of that work, climate model experiments were run with the Community Climate Model of the National Center for Atmospheric Research. In these experiments, a global model with prescribed soil moisture and snow cover was used to simulate climate with and without mountains. Although the model was not integrated through a complete sea-

Geophysical Fluid Dynamics Laboratory–National Oceanic and Atmospheric Administration, Post Office Box 308, Princeton University, Princeton, NJ 08542.

sonal cycle, integrations were made with perpetual January and July insolation in order to study changes in climate in both the winter and summer seasons. There was substantial agreement between the response of the model to changes in orography and climatic changes in the geological record.

We used a GCM with a seasonal cycle to examine the role of mountains in the maintenance of arid and semiarid climates in mid-latitudes of the Northern Hemisphere. While other studies have examined the effects of orography from broader perspectives, we focused specifically on the ability of the model to simulate mid-latitude dry climates and the mechanisms, both atmospheric and hydrologic, by which those climates are maintained. Two experiments were run: one with mountains (M) and another without mountains (NM). The model employs the spectral transform method, in which the horizontal distributions of atmospheric variables are represented by both spherical harmonics and grid-point values (*8*). We retained 30 zonal waves, adopting the so-called rhomboidal truncation. The spacing of the transform grid was 2.25° latitude by 3.75° longitude. Normalized pressure was used as the vertical coordinate, and nine unevenly spaced levels were used for finite differencing. For the computation of radiative transfer, clouds were prescribed, varying only with height and latitude (*9*). Solar radiation at the top of the atmosphere was prescribed, varying seasonally, as was the geographical distribution of sea surface temperature and sea ice. Surface temperatures for land points were computed from a heat balance with the assumption that no heat is stored in the ground. Both snow cover and soil moisture were predicted. The model is similar to the one used by Manabe and Hahn (*10*) except that the M experiment utilized a parameterization of the drag that results from the breaking of orographically induced gravity waves (*11*). Each version of the model was initialized with an isothermal, resting atmosphere and then integrated until a quasi-equilibrium was reached. A subsequent period of 3 years was retained for analysis.

Annual mean soil moisture was used as an indicator of the large-scale patterns of aridity produced by the model (Fig. 1). In the NM experiment, the east-west variation of soil moisture is relatively small, although the east coasts of Asia and North America tend to be slightly wetter than the remainder of those continents. By contrast, soil moisture in the M experiment shows large departures from zonal symmetry. Of particular interest are two mid-latitude regions of low soil moisture: one extending eastward from the Caspian Sea to northwest China, and another just east of the Rocky Mountains in the western interior of North America (*12*). These dry regions correspond quite well to observed regions of dryness and are absent in the NM experiment (*13*).

Annual mean precipitation in the M and NM experiments follows a similar pattern (Fig. 2). In the absence of orography, the smallest amounts are over the Arctic Ocean and in two subtropical regions: the southwestern part of North America and the nearby Pacific, and North Africa and the nearby Atlantic. Precipitation is relatively large over the western portions of the North Atlantic and North Pacific and in a band located between 45°N and 65°N. In the M experiment, precipitation over mid-latitudes has much more east-west variability than in the NM experiment. In addition to the areas of low precipitation in the subtropics and over the polar region, little precipitation falls over the continental interior regions where soil moisture is also small.

Why do these interior regions receive such meager precipitation in the experiment with orography? Some contribution to the dryness of the western interior of North America comes from a relatively simple mechanism. As the prevailing westerly winds in the lower troposphere encounter the extensive north-south barrier of the Rocky Mountains, the air is forced to rise. Condensation and precipitation take place on the upwind side of the mountains, and dry air unfavorable for precipitation subsides on the east side. In addition to this "rain shadow" effect, other mechanisms are involved in maintaining the arid climate of western North America as well as that of interior Eurasia, which has the Tibetan Plateau but lacks a meridional barrier such as the Rocky Mountains.

Much of the precipitation in mid-latitudes is associated with atmospheric disturbances propagating along the polar front, and the preferred locations for disturbance activity are related to the position of stationary waves in the upper troposphere (*14*). Thus another possible explanation for the zonal asymmetry in mid-latitude precipitation in the M experiment is that the presence of orography induces stationary waves that determine the regions of frequent (or infrequent) passage of extratropical disturbances. This hypothesis is explored by examination

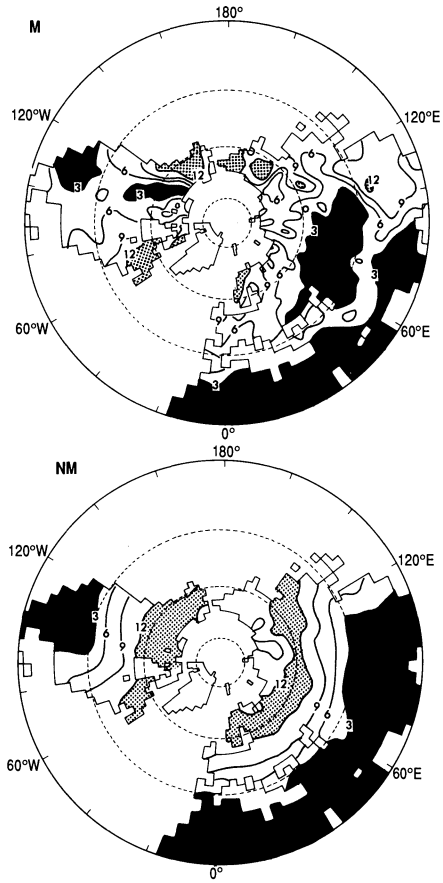

Fig. 1. Annual mean soil moisture (in centimeters) from (**top**) the M and (**bottom**) the NM experiments. Stippling indicates soil moisture >12 cm, whereas solid black shading indicates soil moisture <3 cm. The field capacity of soil moisture in both experiments is 15 cm everywhere. A 1-2-1 smoothing has been applied in both directions to reduce grid-scale variability.

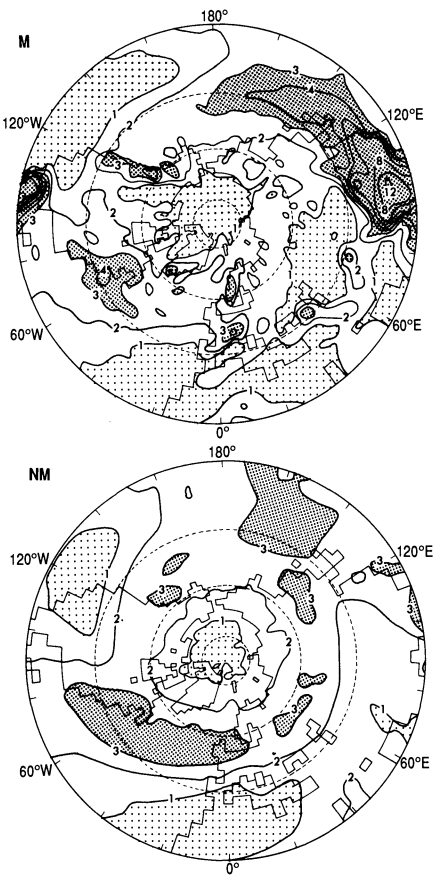

Fig. 2. Annual mean precipitation rate in millimeters per day from the (**top**) M and (**bottom**) NM experiments; smoothing as in Fig. 1.

of a variety of diagnostics of the atmospheric circulation: the 500-mb geopotential height (representing the stream function of geostrophic flow), the 500-mb jet axis, precipitation, and the root-mean-square (rms) of band pass–filtered 500-mb geopotential height (Figs. 3 and 4). Diagnostics for spring are displayed because it is the season in which the continental precipitation belts are best defined in the NM experiment. Autumn and winter atmospheric circulation patterns are qualitatively similar to spring.

In the absence of mountains, stationary waves have relatively small amplitudes and a circumpolar jet axis is present between 45°N and 50°N. A circumpolar band of relatively high transient disturbance activity, indicated by the rms of band pass–filtered 500-mb geopotential height, is located just poleward of this jet axis (*14*). Continental precipitation belts are closely associated with the jet and storm track. In contrast, stationary waves in the M experiment have larger amplitudes, and troughs are situated to the east of the Rocky Mountains and the Tibetan Plateau. This increase in the amplitude of stationary waves in the presence of orography has been noted in earlier studies (*3, 7*). Rather than being almost zonally symmetric, the jet streams in the M experiment are discontinuous and tend to be strongest downstream of the axes of the stationary wave troughs. The storm tracks show a similar discontinuity and are closely aligned with the jet axes. Precipitation tends to be heaviest in the areas downstream of the stationary troughs. In the areas upstream of the troughs, general subsidence prevails, extratropical cyclone activity is relatively weak, and precipitation is light. These features of the mountain-induced stationary waves and jet streams are consistent with theoretical analyses of orographic influences (*15*).

In summer the pattern of stationary waves in the M experiment is quite different from those in the other seasons. Wavelengths are shorter, and the amplitudes are much smaller. Although the North American ridge-trough system associated with the Rocky Mountains is present, the trough downstream of the Tibetan Plateau is absent. Instead, a weaker feature occurs farther west. Despite this difference in position, the distribution of summer mid-latitude precipitation is related to the position of the stationary waves as it is during other seasons. In contrast, circulation features and the distribution of continental precipitation tend to be zonally symmetric during all seasons in the NM experiment.

Another consequence of the changes in atmospheric circulation induced by the presence of mountains is a change in the annual mean vertically integrated moisture transport (not shown). In the NM experiment, zonally symmetric transport occurs throughout the belt from 40°N to 60°N. This flow carries an ample supply of moisture from oceanic sources to the continents. Because soil moisture is relatively high over middle latitudes, evaporation takes place at a substantial fraction of the potential rate. As a result, the land surface is nearly as effective in supplying water vapor to the atmosphere as the ocean surface, and moisture can easily penetrate deep into the continental interiors. In the M experiment, strong eastward transport across the North Pacific and North Atlantic still occurs, but this flow weakens as it enters North America and Europe. The drier land surfaces of the M experiment are not as effective in supplying water vapor to the atmosphere; thus, the moisture transport over the continental interior is reduced.

In order to believe that these mechanisms are responsible for maintaining mid-latitude arid climates, it is necessary to have some confidence in the robustness and realism of the model response. The consistency of our results to those from other studies of orographic effects with different GCMs (*3, 4, 7*) and simple linear models (*15*) suggests that they are relatively robust. Some evidence that similar mechanisms may operate in the real climate system comes from work by others on the evolution of climate on geological time scales. Ruddiman *et al.* accumulated evidence suggesting that much of the uplift in the Tibetan Plateau region and the western United States occurred in the last 5 to 10 million years (*5*). In addition, paleoclimatic data suggest that winters became progressively drier over the northern Great Plains during the last 10 million years and that a general drying of the Eurasian interior took place during a similar period (*6*). The changes in climate between the M and NM experiments are consistent with the paleoclimatic evidence from these regions. Thus we have some confidence that the mechanisms identified here may largely account for mid-latitude aridity.

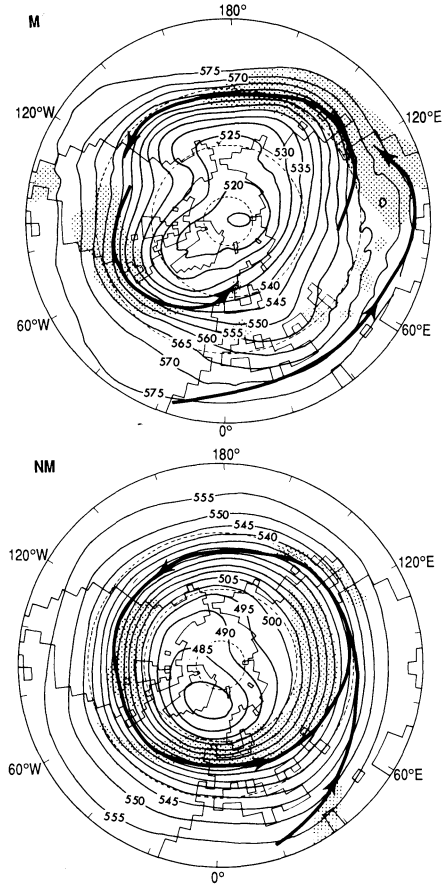

Fig. 3. March-April-May contours of 500-mb geopotential height (in decameters) from (**top**) the M experiment and (**bottom**) the NM experiment. The 500-mb geostrophic wind speed is inversely proportional to the spacing of the height contours, and the thick arrows indicate the position of the jet-stream axis at 500 mb. Stippling indicates precipitation rates >3 mm per day.

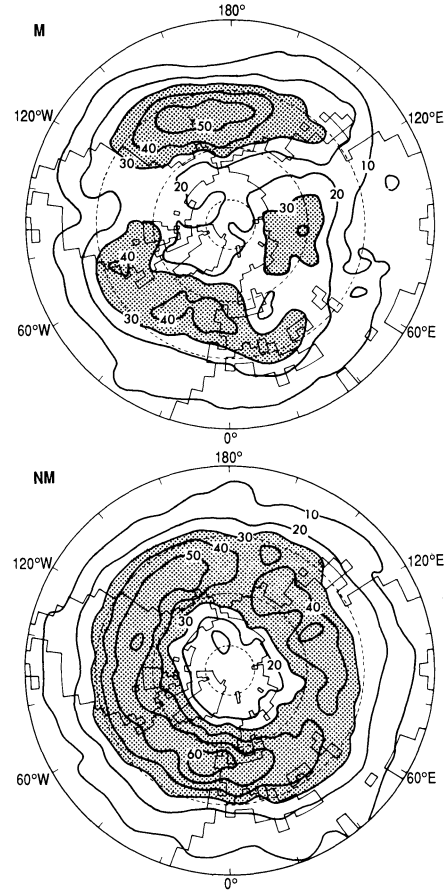

Fig. 4. Root-mean-square (rms) of band pass–filtered 500-mb geopotential height (in meters) from the (**top**) M and (**bottom**) NM experiments. The band pass filter selects disturbances with time scales between 2.5 and 6 days. Stippling indicates values of at least 30 m.

REFERENCES AND NOTES

1. C. W. Thornthwaite, *Geograph. Rev.* **23**, 433 (1933); G. T. Trewartha and L. H. Horn, *An Introduction to Climate* (McGraw-Hill, New York, 1980).
2. Y. Mintz, *World Meteorol. Org. Tech. Note 66* (1965); A. Kasahara and W. M. Washington, *J. Atmos. Sci.* **28**, 657 (1971); A. Kasahara, T. Sasamori, W. M. Washington, *ibid.* **30**, 1229 (1973); T. Tokioka and A. Noda, *J. Meteorol. Soc. Jpn.* **64**, 819 (1986).
3. S. Manabe and T. B. Terpstra, *J. Atmos. Sci.* **31**, 3 (1974).
4. S. Manabe and J. L. Holloway, Jr., *J. Geophys. Res.* **80**, 1617 (1975).
5. W. F. Ruddiman *et al.*, *ibid.*, in press.
6. W. F. Ruddiman and J. E. Kutzbach, *ibid.*, in press.
7. J. E. Kutzbach *et al.*, *ibid.*, in press.
8. C. T. Gordon and W. F. Stern, *Mon. Weather Rev.* **110**, 625 (1982); W. Bourke, *ibid.* **102**, 687 (1974).
9. The M experiment was also performed with another version of the model in which cloud cover is predicted and its radiative effect incorporated according to a methodology described by Wetherald and Manabe [*J. Atmos. Sci.* **44**, 1397 (1988)]. The arid climates of mid-latitudes obtained from this experiment are similar to those obtained from the present study except that they are slightly drier.
10. S. Manabe and D. G. Hahn, *Mon. Weather Rev.* **109**, 2260 (1981).
11. The formulation of mountain gravity-wave drag at subgrid scale that we adopted was developed by Y. Hayashi and is similar to that described by R. T. Pierrehumbert [in *Observation, Theory, and Modelling of Orographic Effects* (European Center for Medium Range Forecasting, Reading, 1987), vol. 1, pp. 251–282]. The magnitude of the surface mountain drag in the M experiment was adjusted to make the latitudinal profile of zonally averaged sea-level pressure for January realistic. Without gravity-wave drag, the tropospheric wind and near-surface climate in the middle latitudes of the Northern Hemisphere tend to be too zonal (although not as zonal as the NM experiment). Thus the effect of subgrid-scale mountain drag is essential for satisfactory simulation of the dry climates in the middle latitudes of the Northern Hemisphere. Because the drag is proportional to the subgrid-scale topographic variance, it was not incorporated in the NM experiment.
12. Because of the finite horizontal resolution of the model and the effects of spectral truncation, the complex mountain topography of the western United States was represented as a broad ridge with a maximum elevation of ~3 km. Because its central axis parallels the Rocky Mountains, we will refer to this feature by that name.
13. Although no observed soil moisture data are used for comparison, the correspondence between the distribution of dry climates in the M experiment and the observed distribution is evident when the climate classification system developed by Köppen is used. In this scheme monthly mean temperature and precipitation are used to determine a climatic classification designed to correspond to the prevailing vegetation. This scheme is described in detail by H. H. Lamb [in *Climate: Present, Past and Future* (Methuen, London, 1972), pp. 509–514]. On the basis of this system, the distribution of desert and steppe climates (Köppen's category B) from the M experiment is quite similar to that observed in the mid-latitude Northern Hemisphere; this similarity implies that the model's simulation of temperature and precipitation is realistic.
14. The close relation between transient disturbance activity and the rms of band pass–filtered 500-mb geopotential height in the real atmosphere has been discussed by M. L. Blackmon *et al.* [*J. Atmos. Sci.* **34**, 1040 (1977)] and M. L. Blackmon and N.-C. Lau [*ibid.* **37**, 497 (1980)].
15. B. Bolin, *Tellus* **2**, 184 (1950); S. Nigam, I. M. Held, S. W. Lyons, *J. Atmos. Sci.* **45**, 1433 (1988).
16. We thank I. M. Held, Y. Kushnir, J. Mahlman, and C. Milly for constructive reviews of the first draft of this manuscript. The comments of the anonymous reviewers were also valuable.

29 August 1989; accepted 1 November 1989

Allometric Scaling in the Earliest Fossil Bird, *Archaeopteryx lithographica*

MARILYN A. HOUCK, JACQUES A. GAUTHIER, RICHARD E. STRAUSS

***Archaeopteryx* is almost universally considered a primitive bird. Debate persists, however, about the taxonomic assignment of the six skeletal fossils. Allometric scaling of osteological data shows that all specimens are consistent with a single growth series. The absence of certain bone fusions suggests that no specimen is full-grown. Allometric patterns, as compared to growth gradients of other dinosaurs, extant ectotherms, and extant endotherms, suggest that *Archaeopteryx* was likely a homeothermic endotherm with rapid growth and precocial abilities for running and flying. Multivariate allometric models offer a significant potential for interpreting ontogenetic patterns and phylogenetic trends in the fossil record.**

Archaeopteryx REPRESENTS A RARE transitional form in the fossil record (*1, 2*). During the past 130 years of scrutiny and sustained controversy, the six described specimens have been variously parceled among six different genera and nine different species (*3*). The most recent taxonomic revision occurred in 1985 (*4*) and the most recent disclosure of a new specimen in 1988 (*5*).

Contention about the status of these specimens has persisted because of the inconsistencies in relative sizes and proportions and the lack of unambiguous diagnostic characters (*6*). Because previous attempts have not resolved the taxonomic issues, we reexamined the variability among the specimens with an exponential allometric (growth-series) model. The allometric model is useful in interpreting growth patterns among developmental stages within a taxon (*7, 8*), and divergent growth patterns can distinguish multiple taxa (*9*). Growth patterns differ among taxa either because the relative growth rates (allometries) of individual characters differ or because the timing (heterochrony) of structural development differs. The most divergent allometric (or heterochronic) variables can contribute to the evolutionary separation of closely related taxa within a phylogeny (*9*).

To apply an allometric growth model as an alternative hypothesis against which to test patterns of phylogenetic change (*10*), we first needed to determine whether the specimens represented elements of a consistent progression, differing only in absolute size (age). Nine major skeletal components, and available dimensions for maxillary and premaxillary teeth, were examined as simple functions of femur length, a commonly used index of body size in birds. All linear regressions resulted in high correlation coefficients, consistent with a single series (Fig. 1).

Skeletal fusions, an independent qualitative line of evidence, also support the interpretation of ontogenetic stages. All full-grown coelurosaurs (*11*) are known to have had a variety of skeletal fusions that were complete in full-grown adults (*12*). Even though a substantial size range exists among the six *Archaeopteryx* specimens (the largest being twice the size of the smallest), no specimen had a full complement of these age-related fusions. The smallest specimen (Eichstätt) had no such fusions. The limited extent of skeletal fusions suggests that none of the specimens was full-grown.

Growth and the development of flight feathers are frequently correlated in extant birds. A full complement of wing and tail feathers existed in the Eichstätt specimen, despite its small size. This might suggest that the Eichstätt specimen was a full-grown member of sympatric (but smaller) species, but this is not a necessary conclusion. Some megapodes have a full complement of flight feathers and are fully homeothermic immediately upon hatching (*13*), and most volant precocial birds can fly short distances within the first week of post-hatching development (*14*). Thus, the development of feathers in the smallest specimen is not incompatible with a single-species growth series. Further, it is consistent with a hypothesis that precocial flight and thermoregulation are ancestral for living birds.

The parsimonious conclusion is that all six fossils are consistent with a single size-series and that none of the specimens were fully grown (*15*). Therefore it is appropriate to use an allometric growth model to examine changes in skeletal proportions that accompany differences in size. The growth dynamics of *Archaeopteryx* can then be compared with related theropod lineages in terms of ancestral affinities and context with extant taxa. Such comparative allometric ap-

M. A. Houck and R. E. Strauss, Department of Ecology and Evolutionary Biology, University of Arizona, Tucson, AZ 85721.
J. A. Gauthier, Department of Herpetology, California Academy of Sciences, Golden Gate Park, San Francisco, CA 94118.